2025 IEEE/SICE International Symposium on System Integration (SII)
January 21-24, 2025, Munich, Germany

Dynamic Behavior Analysis of Copper Wire for Motor Coil Manufacturing

Masato Nagano, Hidefumi Wakamatsu, Yoshiharu Iwata, Hironori Suzuki, Takumi Nakaue, and Takahiro Tanaka

***Abstract*—Manufacturing defects such as bulging, or overlap can occur when winding copper wires by winding machines. In this paper, the method of dynamic behavior analysis of copper wire is proposed. First, the deformation of copper wire on physical constraints is formulated considering elastoplastic expansion, contraction, bending, and torsional deformation. Next, supplying of the copper wire is modeled to reduce computational load and unnecessary vibration of the copper wire in the simulation. Finally, the dynamic behavior of the copper wire is simulated when it is wound by the winding machine. The simulation results showed that the bulging problem is related to core rotation speed and the tension of copper wire supplied.**

I. Introduction

In the electrical machinery manufacturing industry, the demand for electric motor coils is increasing due to such as the expansion of the electric vehicle market[1]. Therefore, efficient production of motor coils is important.

The efficiency of permanent magnet motors is closely related to manufacturing engineering. By winding at high density, coil resistance can be reduced, and energy losses due to coil heating can also be reduced. A lot of research on motor winding technology has been actively conducted, such as winding using dividing stator core structures [2] and arraying winding technology for continuous rectangular wire concentrated wound coils[3]. However, manufacturing defects such as bulging and overlap of copper wires, which reduce coil density, can occur in the winding process with winding machines. When such manufacturing defects occur, rewinding of copper wires must be performed, leading to decreased productivity. Furthermore, since the cause of such defects is not clearly understood, their solution depends on the experience of the machine operators. Therefore, this study aims to predict such defects in advance with simulation of the behavior of copper wires during the motor coil winding process.

Prior research related to this study can be broadly divided into studies on deformation analysis of linear objects and studies on simulating the plastic deformation of metals. Fully nonlinear 3D modeling of linear objects by Simo et al., which incorporates transverse shear deformation and torsional warping deformation, considers large deformations using a curvilinear coordinate system[4]. This approach enables the handling of the motion of flexible objects. The Absolute Nodal Coordinate (ANC) method represents large deformations of flexible structures using nonlinear finite elements[5,6]. Research using the ANC method has been prevalent in recent years[7], but it faces the issue of high computational load, so there are few studies on handling the contact between ANC elements or the contact between objects and ANC elements. Wu et al. and Zhang et al. have predicted the amount of spring-back in the bending process of metal wires, such as copper wires, using the finite element method[8,9]. However, the above-mentioned studies do not provide predictions for wire elastoplastic expansion and torsion. Therefore, in this paper, it is proposed that a dynamic analysis method using a discrete model representing the elastoplastic expansion, contraction, bending, and torsional deformations of copper wires. As a first step, the *bulging* of copper wires as shown Fig. 1 is aimed to be predicted with our proposed method. It is a phenomenon where the winding loosens during the winding process, causing the copper wire to float up from the iron core.

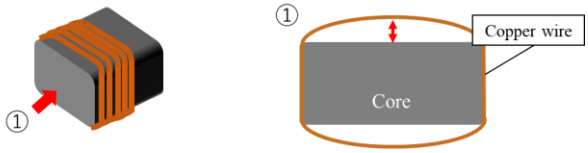

(a) Coil after partial winding. (b) The bulging phenomenon.

Figure 1. The bulging of copper wires.

II. Modeling of Copper Wire

A. Formulation of motion

First, a copper wire is modeled to perform dynamic simulation. The following three assumptions are made for the simulation model in this paper. At first, a finite number of mass points are connected by springs to represent a copper wire as a discrete model. Second, four deformation characteristics of a copper wire, such as the expanding, contracting, bending, and torsional deformation, are considered. Finally, copper wire is not deformed in the cross-sectional direction and the cross-sectional shape of copper wire is always circular.

Based on the above assumptions, a copper wire is modeled in Fig. 2. A copper wire is assumed to have length L, line density ρ, and radius r of the cross section. Since the copper wire is modeled discreetly in this paper, it is represented by n mass points and (n-1) line segments joining them. Therefore, the mass of each mass point M and the natural length of a line segment l are defined as (1).

$$M = \rho L/n, \qquad l = L/(n-1) \tag{1}$$

Masato Nagano, Hidefumi Wakamatsu, and Yoshiharu Iwata are with Dept. of Materials and Manufacturing Science, Graduate School of Eng., Osaka University, Yamadaoka 2-1, Suita, Osaka 565-0871, Japan (e-mail: {masato.nagano, wakamatu, iwata} @mapse.eng.osaka-u.ac.jp).

Takumi Nakaue, Takahiro Tanaka, and Hironori Suzuki are with Component Production Engineering Center, Mitsubishi Electric Corporation, 8-1-1, Tsukaguchi-Honmachi, Amagasaki City, Hyogo 661-8661, Japan (email:{ suzuki.hironori@ap, nakaue.takumi@ea, tanaka.takahiro@dx } .mitsubishielectric.co.jp).

The coordinates of each mass point are expressed in the spatial coordinate system $O-xyz$, so the coordinates of the i-th mass point are $\boldsymbol{p}_i = [x_i \quad y_i \quad z_i]^{\mathrm{T}}$ $(1 \le i \le n)$. The expanding / contracting and bending deformation are formulated in this coordinate system. Additionally, an object coordinate system $P_i - \xi_i\eta_i\zeta_i$ is set up to model torsional deformation. The object coordinate system rotates due to the deformation of the copper wire, which is represented by quaternion $\boldsymbol{q}_i = [q_{0,i} \quad q_{1,i} \quad q_{2,i} \quad q_{3,i}]^{\mathrm{T}}$. However, it is important to note that a constraint that the ζ_i-axis is parallel to the straight spring must be satisfied even if the object coordinate system is rotated. In this paper, this constraint is defined as *a rotational constraint*. Then, rotation around the ζ_i-axis corresponds to the torsion of a copper wire.

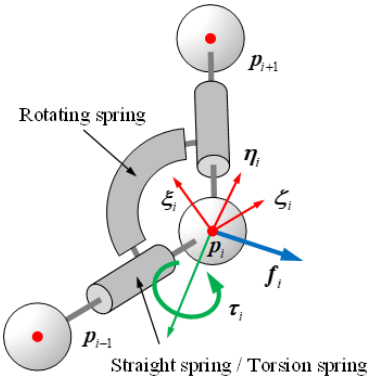

Figure 2. Model diagram of a copper wire.

The equations of motion for the translation and rotation of the i-th mass point are expressed as (2).

$$M\ddot{\boldsymbol{p}}_i = \boldsymbol{f}_i, \qquad \frac{2}{5}Mr^2 Q_i \ddot{\boldsymbol{q}}_i = \boldsymbol{\tau}_i \tag{2}$$

Here, $\boldsymbol{f}_i$ represents the forces from the straight springs and rotating springs, and $\boldsymbol{\tau}_i$ represents the torque from the torsional springs connected to the mass point. Q_i is defined as (3).

$$Q_i = \begin{bmatrix} -q_{1,i} & q_{0,i} & q_{3,i} & -q_{2,i} \\ -q_{2,i} & -q_{3,i} & q_{0,i} & q_{1,i} \\ -q_{3,i} & q_{2,i} & -q_{1,i} & q_{0,i} \end{bmatrix} \tag{3}$$

B. *Consideration of constraints*

We consider constraints that must be satisfied during dynamic deformation. First, quaternions must be satisfied the following constraint in general.

$$q_{0,i}{}^2 + q_{1,i}{}^2 + q_{2,i}{}^2 + q_{3,i}{}^2 = 1 \tag{4}$$

Next, to satisfy the rotational constraint, the straight spring between the $(i-1)$-th point and the i-th point must be orthogonal to the ξ_i-axis and the η_i-axis. Thus, the following equations must be satisfied.

$$(\boldsymbol{p}_i - \boldsymbol{p}_{i-1}) \cdot \boldsymbol{\xi}_i = 0, \qquad (\boldsymbol{p}_i - \boldsymbol{p}_{i-1}) \cdot \boldsymbol{\eta}_i = 0 \tag{5}$$

In this paper, the constraint stabilization method[10] is applied to satisfy all constraints. The constraint stabilization method solves the following differential equation in conjunction with the equation of motion when the constraint equation to be satisfied is $R = 0$.

$$\ddot{R} + 2\nu\dot{R} + \nu^2 R = 0 \tag{6}$$

Equation (6) can be transformed to a second-order differential equation of variables x_i, y_i, z_i, $q_{0,i}$, $q_{1,i}$, $q_{2,i}$, or $q_{3,i}$. Then, by solving it simultaneously with (2), the behavior of the copper wire can be calculated with considering these constraints.

C. *Modeling of elastoplastic deformation*

The forces and moments on the right side of (2) are mainly applied to each mass point from various springs. They are formulated in this section.

In this paper, assuming the copper wire as a hardening elastoplastic material, the plastic hysteresis in expanding/contracting, bending, and torsional deformations is modeled using two straight lines, as shown in Fig. 4. The plastic hysteresis shifts as shown in Fig. 5(a) to 5(c).

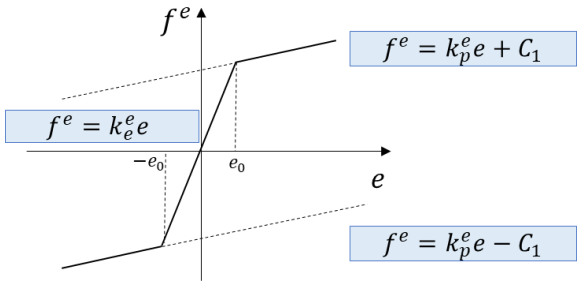

Figure 3. Plastic hysteresis approximated by two lines.

First, it is formulated that the force exerted on the mass point by the straight springs. The expansion or contraction of the straight springs is defined as e, and the force exerted by the expansion spring on the connected mass point is denoted as f^e. The spring constant during elastic deformation is k_e^e, during plastic deformation is k_p^e. The yield point in expanding deformation, namely, the expansion at which elastic deformation transits to plastic deformation is referred to as e_{ye}. The yield point in contracting deformation, namely, the contraction at which elastic deformation transits to plastic deformation is referred to as e_{yc}. Let a be the expansion at which the straight spring first yields, and C_1 is defined as $C_1 = a(k_e^e - k_p^e)$.

(a) In case that $e_{yc} \le e \le e_{ye}$, f^e is represented as follows:

$$f^e = -k_e^e(e - e_{ye}) + (k_p^e e_{yc} + C_1). \tag{7}$$

In this case, the point (e, f^e) exists on the line with a slope of k_e^e. The yield points, e_{yc} and e_{ye}, are not updated.

(b) In case that $e_{ye} < e$, f^e is represented as follows:

$$\boldsymbol{f^e = -k_p^e e + C_1}. \tag{8}$$

In this case, the point (e, f^e) exists on the line of $f^e = -k_p^e e + C_1$. Then, the yield points, e_{yc} and e_{ye}, move in the

positive direction along the horizontal axis and e_{ye} is replaced as e.

(c) In case that $e < e_{yc}$, f^e is represented as follows:

$$f^e = -k_p^e e - C_1. \tag{9}$$

In this case, the point (e, f^e) exists on the line of $f^e = -k_p^e e - C_1$. Then, the yield points, e_{yc} and e_{ye}, move in the negative direction along the horizontal axis and e_{yc} is replaced as e.

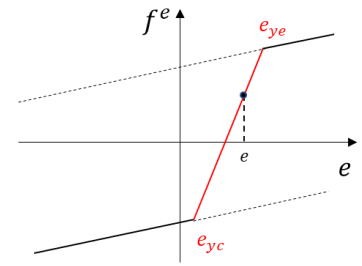

e_{ye} *and* e_{yc} are not updated

(a) $e_{yc} \le e \le e_{ye}$

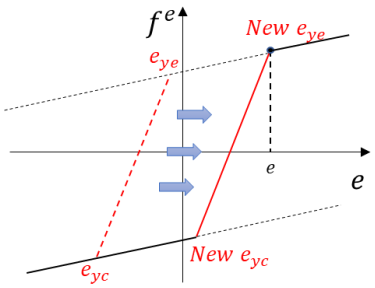

e_{ye} *and* e_{yc} are updated

(b) $e_{ye} < e$

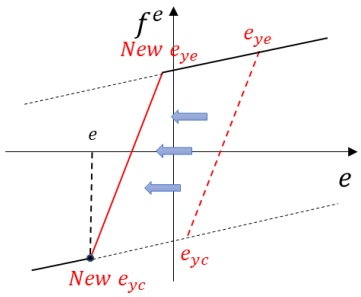

e_{ye} *and* e_{yc} are updated

(c) $e < e_{yc}$

Figure 4. Absolute value of f^e in cases (a)-(c).

Next, plastic deformation in bending is considered. Let α be the rotation angle of the rotational spring, and m^b be the magnitude of the moment generated by the rotational spring around the mass point. The spring constant during elastic deformation is denoted as k_e^b, and that during plastic deformation k_p^b. The yield point in bending deformation clockwise is referred to as α_{yc} and that in bending deformation counterclockwise α_{ya}. Let b be the angle at which the rotational spring first yields, and C_2 is defined as $C_2 = b(k_e^b - k_p^b)$. The plastic hysteresis in bending deformation is modeled in the following cases (a) to (c) as similar to that in the expanding/contracting deformation:

(a) In case that $\alpha_{yc} \le \alpha \le \alpha_{ya}$:

$$m^b = k_e^b(\alpha - \alpha_{yc}) + (k_p^b \alpha_{ya} + C_2). \tag{10}$$

(b) In case that $\alpha_{ya} < \alpha$:

$$m^b = -k_p^b \alpha + C_2. \tag{11}$$

(c) In case that $\alpha < \alpha_{yc}$:

$$m^b = -k_p^e \alpha - C_2. \tag{12}$$

In this paper, the moment m^b is divided by the length of the straight spring and converted into the force acting on the mass points at both ends of the rotational spring.

Finally, plastic deformation in torsional deformation is considered. Let θ be the rotation angle of the torsional spring and m^t be the magnitude of the moment generated by the torsional spring. The spring constant during elastic deformation is denoted as k_e^t, and that during plastic deformation k_p^t. The yield point in torsional deformation clockwise is referred to as θ_{yc}, which is a negative value, and that in torsional deformation counterclockwise θ_{ya}, which is a positive value. Let c be the angle at which the torsional spring first yields, and C_3 is defined as $C_3 = c(k_e^t - k_p^t)$. The plastic hysteresis in torsional deformation is modeled in the following cases (a) to (c) as similar to that in the bending deformation:

(a) In case that $\theta_{yc} \le \theta \le \theta_{ya}$:

$$m^t = k_e^t(\theta - \theta_{yc}) + (k_p^b \theta_{ya} + C_3). \tag{13}$$

(b) In case that $\theta_{ya} < \theta$:

$$m^t = -k_p^t \theta + C_3. \tag{14}$$

(c) In case that $\theta < \theta_{yc}$:

$$m^t = -k_p^t \theta - C_3. \tag{15}$$

The forces obtained from $\boldsymbol{f^e}$ and m^b are substituted into $\boldsymbol{f}_i$, and m^t is substituted into $\boldsymbol{\tau_i}$ in (2).

III. Modeling of Contact and Friction

To accurately simulate the process of copper wire winding around an iron core, it is essential to consider both the contact interactions between the copper wire and the iron core and the resulting frictional forces. In this paper, a virtual spring mechanism on the surface of the iron core is employed to represent the normal force exerted when a mass point encounters it, as illustrated in Fig. 3. The velocity of the j-th plane constituting the iron core is denoted as $\boldsymbol{u}_j$, and the unit normal vector is denoted as $\boldsymbol{n}_j$. The vertical relative velocity $\boldsymbol{v}_{v,i,j}$ and the horizontal relative velocity $\boldsymbol{v}_{h,i,j}$ of the i-th mass point with respect to the j-th plane are expressed by the following equations.

$$\boldsymbol{v}_{v,i,j} = \{\boldsymbol{n}_j \cdot (\dot{\boldsymbol{p}}_i - \boldsymbol{u}_j)\}\,\boldsymbol{n}_j \tag{16}$$

$$\boldsymbol{v}_{h,i,j} = (\dot{\boldsymbol{p}}_i - \boldsymbol{u}_j) - \boldsymbol{v}_{v,i,j} \tag{17}$$

Let $h_{i,j}$ be the penetration depth of the mass point into the plane and k_j be the spring constant of the virtual spring on the plane.

If $\boldsymbol{v}_{h,i,j} \neq 0$, the mass point is subjected to normal force and kinetic friction force, and the equations of motion are as follows.

$$m\ddot{\boldsymbol{p}}_i = \boldsymbol{f}_i + k_j h_{i,j}\boldsymbol{n}_j - \mu_d k_j h_{i,j}\frac{\boldsymbol{v}_{h,i,j}}{|\boldsymbol{v}_{h,i,j}|} \tag{18}$$

If $\boldsymbol{v}_{h,i,j} = 0$, the equations of motion are as follows.

$$\boldsymbol{f}_{v,i,j} = (\boldsymbol{n}_j \cdot \boldsymbol{f}_i)\,\boldsymbol{n}_j, \qquad \boldsymbol{f}_{h,i,j} = \boldsymbol{f}_i - \boldsymbol{f}_{v,i,j} \tag{19}$$

$$m\ddot{\boldsymbol{p}}_i = \boldsymbol{f}_{h,i,j} + k_j h_{i,j}\boldsymbol{n}_j \tag{20}$$

At this time, due to static friction, the mass point remains stationary in the horizontal direction of the plane. If $\boldsymbol{f}_{h,i,j}$ exceeds the maximum static friction force, the calculation is redone assuming the mass point starts moving.

If $\boldsymbol{p}_i$, $\boldsymbol{q}_i$ $\dot{\boldsymbol{p}}_i$, and $\dot{\boldsymbol{q}}_i$ at time t are given, $\ddot{\boldsymbol{p}}_i$ and $\ddot{\boldsymbol{q}}_i$ at time t can be obtained by solving the equation of motion described by (2). From these second-order differential values, $\boldsymbol{p}_i$, $\boldsymbol{q}_i$, $\dot{\boldsymbol{p}}_i$, and $\dot{\boldsymbol{q}}_i$ at time $t+\Delta t$ can be predicted by applying an appropriate numerical solution. By repeating this process, the dynamic deformation of the copper wire can be predicted. In this paper, the Runge-Kutta-Fehlberg method, which allows Δt to be changed, is used as the numerical solution method.

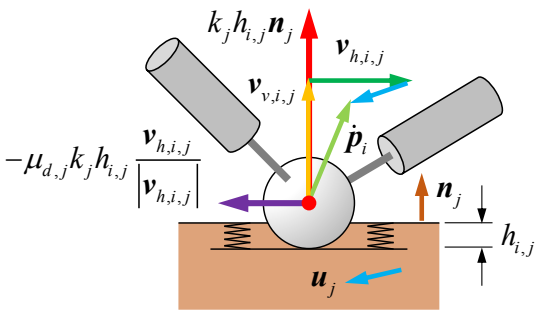

Figure 5. Model diagram of contact and friction.

IV. Modeling of Supplying Copper Wire

To predict the dynamic behavior of a long copper wire, the equations of motions concerning a large number of mass points must be solved repeatedly. It leads to a heavy computational load. To reduce such a load, it is desirable to model only the region of interest rather than the entire winding machine. Therefore, it is modeled that the behavior of a copper wire being pulled into the simulation area from the outside due to applied forces.

First, it is assumed that a constant tension is applied to a copper wire outside the area. This tension is represented by $\boldsymbol{F}_T$. The coordinates of a supply port are denoted by $\boldsymbol{p}_s$. Note that $\boldsymbol{p}_s$ depends on time t because the supply port can move.

The segment passing through the supply port is defined as the *boundary segment*. It is assumed that the boundary segment is connected to the n-th mass point and the (n+1)-th mass point, which exists outside the simulation area as shown in Fig. 6(a). Furthermore, the boundary segment is assumed to be parallel to the supply port direction and be expanded due to the constant tension. Then, the coordinates of the (n+1)-th mass point are described as follows:

$$\boldsymbol{p}_{n+1} = \boldsymbol{p}_n + \left(l + \frac{|\boldsymbol{F}_T|}{k^e}\right)\boldsymbol{\zeta}_n \tag{21}$$

In this paper, it is imposed a constraint that the direction $\boldsymbol{\zeta}_{n+1}$ of the boundary segment must coincide with that $\boldsymbol{\zeta}_n$ of its adjacent segment. This constraint is represented as follows because the boundary segment must be on the supply port:

$$\begin{cases} (\boldsymbol{p}_n - \boldsymbol{p}_s)\cdot\boldsymbol{\xi}_n = 0 \\ (\boldsymbol{p}_n - \boldsymbol{p}_s)\cdot\boldsymbol{\eta}_n = 0 \\ (\boldsymbol{p}_{n+1} - \boldsymbol{p}_s)\cdot\boldsymbol{\xi}_n = 0 \\ (\boldsymbol{p}_{n+1} - \boldsymbol{p}_s)\cdot\boldsymbol{\eta}_n = 0 \end{cases} \tag{22}$$

Constraints as described in (22) can be satisfied by applying the constraint stabilization method.

When the (n+1)-th mass point passes through the supply port as the copper wire is pulled in, it is generated that a new boundary segment and the (n+2)-th mass point corresponding to a terminal one of the new boundary segment as shown in Fig. 6(b). The coordinates of the (n+2)-th mass point are described in (21) and constraints represented by (22) are imposed on the new boundary segment.

By repeating the above process, the copper wire supply can be simulated.

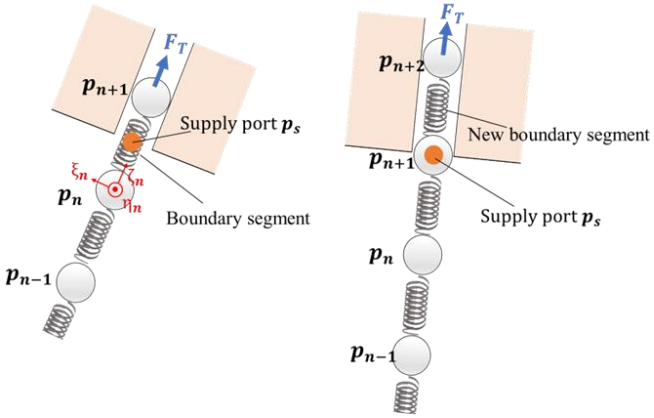

(a) Boundary segment between $\boldsymbol{p}_n$ and $\boldsymbol{p}_{n+1}$.

(b) Adding new boundary segment.

Figure 6. Model diagram of supplying copper wire

V. Case Study

Using the methods described above, the behavior of the copper wire winding around the iron core is simulated. Although the actual shape of the iron core is closer to a rectangular prism with rounded corners, for simplicity, it is considered as four cylinders in this simulation. Table 1 shows the material properties used in the simulation.

A constraint is applied to fix one end of the copper wire to a cylinder, allowing the copper wire to wind around the iron

TABLE 1. PROPERTIES USED IN SIMULATION.

Copper wire diameter	Ø 1.0 mm
Line density	7.02×10^5 kg/m
Elongation rigidity in elastic deformation	4.89×10^4 N
Elongation rigidity in plastic deformation	1.10×10^3 N
Bending rigidity in elastic deformation	3.06×10^{-3} N · m^2
Bending rigidity in plastic deformation	1.13×10^{-4} N · m^2
Torsional rigidity in elastic deformation	4.32×10^{-3} N · m^2
Torsional rigidity in plastic deformation	9.0×10^{-5} N · m^2
Coefficient of static friction	0.23
Coefficient of kinetic friction	0.17
Cylinder diameter of iron core	Ø 5.0 mm

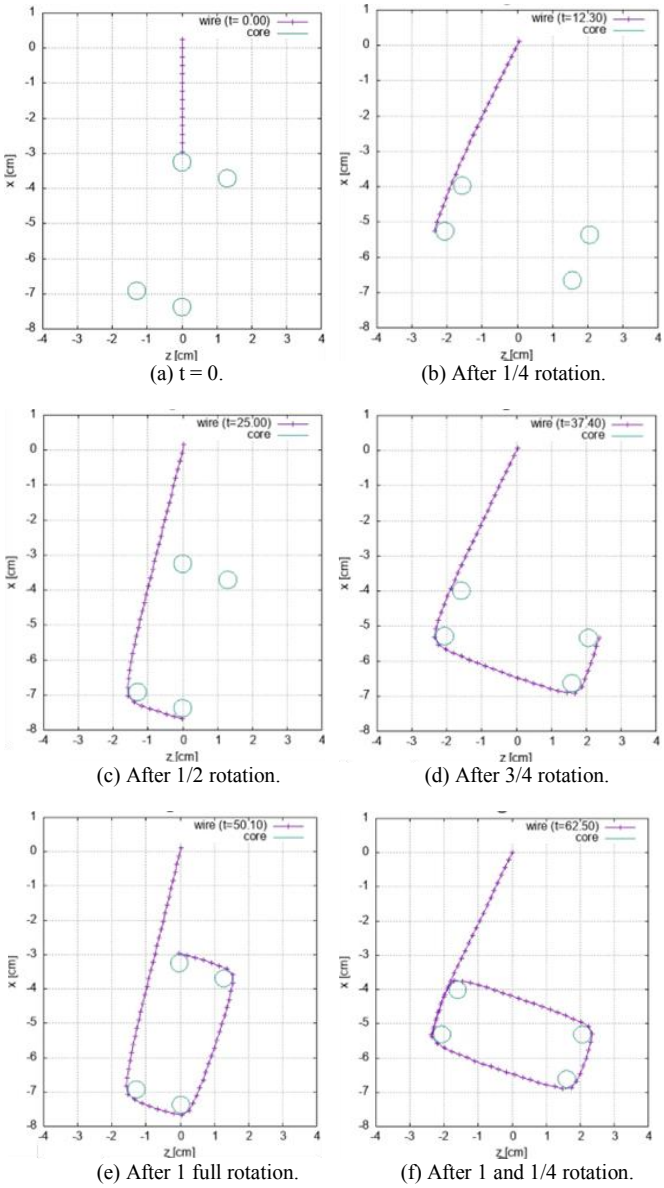

(a) t = 0. (b) After 1/4 rotation.

(c) After 1/2 rotation. (d) After 3/4 rotation.

(e) After 1 full rotation. (f) After 1 and 1/4 rotation.

Figure 7. An example of simulation results.

core as the core rotates. This constraint can be satisfied by applying the constraint stabilization method. As the iron core rotates, the supply port moves along the axial direction of cylinders. As the result, the copper wire is wound in a spiral shape. For the purpose of examining the degree of bulging, a two-dimensional representation is used in this case. Fig. 7 shows an example of the simulation results.

As shown in Fig. 7, one end of the copper wire is always fixed to the iron core. The direction of the supply port changes following the rotation of the rectangular iron core. The copper wire is continuously pulled in as the iron core rotates. The wire is wound around the iron core without interference. Consequently, it is concluded that the process of the copper wire winding around the iron core was successfully simulated.

Next, the bulging is investigated by varying the rotation speed of the iron core and the tension of the copper wire. It was selected that 600 rpm and 1200 rpm as the rotation speed, and 30 N and 70 N as the tension. Fig.8 shows the state of the copper wire after 1 and 3/4 rotations for each combination of parameters. Comparing Fig. 8(a) to Fig. 8(b) and Fig.8(c) to Fig.8(d), it was found that the bulging becomes larger as the tension decreases. Although the effect is smaller compared to tension, differences in bulging were also observed due to the rotation speed of the iron core.

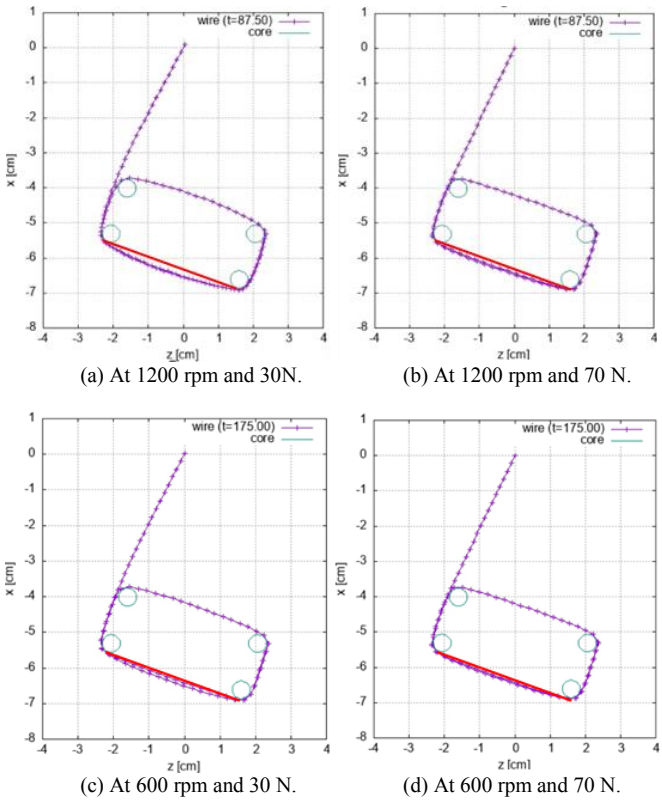

(a) At 1200 rpm and 30N. (b) At 1200 rpm and 70 N.

(c) At 600 rpm and 30 N. (d) At 600 rpm and 70 N.

Figure 8. The state of the copper wire after 1 and 3/4 rotations.

VI. CONCLUSION

This study aims to predict the shape of the copper wire during the motor coil manufacturing process and proposes a method for predicting the dynamic behavior of the copper wire as it winds around the iron core during the winding process. Simulation results showed that varying the rotation

speed of the iron core and the supply tension of the copper wire can change the degree of bulging. Additionally, it was found that the bulging is smaller at lower rotation speeds and larger tensions, consistent with real-world phenomena. In the future, the validity of the proposed method will be verified through comparison with actual machines, and the simulation results will be applied to the actual motor coil manufacturing process.

REFERENCES

[1] Shinichi Iizuka, "Technical Trend of Magnet Wires Supporting High-Performance Magnetic", Journal of the Japan society of Polymer Processing, vol. 20, No.12, 2008, pp.864-868

[2] Hiroyuki Akita, Yuji Nakahara, Nobuyuki Miyake, Tomoaki Oikawa, "New Core Structure and Manufacturing Method", IEEE 38th IAS Annual Meeting on Conference Record of the Industry Applications Conference, 2003

[3] Takashi Ishigami, "Arraying Winding Technology for Continuous Rectangular Wire Concentrated Wound Coils", IEEJ Transactions on Industry Applications, Vol.138 No.8 pp.706-712

[4] Simo, J.C. and Vu-Quoc, L, "A geometrically exact rod model incorporating shear and torsion warping deformation", International Journal of Solids and Structures, Vol.27, No.3, 1991, pp.371- 393

[5] A.A. Shabana, "Dynamics of Multibody Systems", Cambridge University Press (2013)

[6] A.A. Shabana, H.A. Hussien, J.L. Escalona, "Application of the Absolute Nodal Coordinate Formulation to Large Rotation and Large Deformation Problems", Journal of Mechanical Design, 1998, 120(2), pp.188-195

[7] J. Gerstmayr, Hiroyuki Sugiyama, Aki Mikkola, "Review on the Absolute Nodal Coordinate Formulation for Large Deformation Analysis of Multibody Systems", Journal of Computational and Nonlinear Dynamics, 2013, 8(3), 031016

[8] ZHANG Xian, ZHAO Zhang Feng, ZHONG Jiang, "Establishment and Research on Spring-back Mathematical Model of Wire Roll Bending Process", light industry machinery, China 2010

[9] Liu Jin Wu, He Yong Xiang, "Analysis of Re-spring Process of Ideal Elastic-plastic Material and Calculation of its Re-spring Bending Moment", Metal Forming Technology, China 2001

[10] J. Baumgarte, "Stabilization of Constraints and Integrals of Motion in Dynamical Systems", Computer Methods in Applied Mechanics and Engineering, vol.1, no.1, 1972, pp.1-16.